Study on an advanced adsorption desalination cycle with evaporator-condenser heat recovery circuit

Thu, Kyaw
Department of Mechanical Engineering, National University of Singapore

Saha, Bidyut Baran
Mechanical Engineering Department, Faculty of Engineering, Kyushu University

Chakraborty, Anutosh
Department of Mechanical and Areospace Engineering, Nanyang Technological Institute

Chun, Won Gee
Department of Nuclear and Energy Engineering, Cheju National University

他

出版情報：International Journal of Heat and Mass Transfer. 54 (1/3), pp.43-51, 2011-01-15. Elsevier
バージョン：

Study on an Advance Adsorption Desalination Cycle with Evaporator-Condenser Heat Recovery Circuit

Kyaw Thu[1], Bidyut Baran Saha[2,*], Anutosh Chakraborty[3], Won Gee Chun[4] and Kim Choon Ng[1,*]

[1]Department of Mechanical Engineering, National University of Singapore, 9 Engineering Drive 1, Singapore 117576

[2]Mechanical Engineering Department, Faculty of Engineering, Kyushu University, 744 Motooka, Nishi-ku, Fukuoka-shi, Fukuoka 819-0395, Japan

[3]Department of Mechanical and Areospace Engineering, Nanyang Technological Institute, 50 Nanyang Avenue, Singapore 639798

[4]Department of Nuclear and Energy Engineering, 66 Jejudaehakno, Jejusi, Cheju National University, Korea

***Corresponding author e-mails:** saha@mech.kyushu-u.ac.jp (B.B. Saha)
mpengkc@nus.edu.sg (K.C. Ng)

Abstract

This paper presents the results of an investigation on the efficacy of a silica gel-water based advance adsorption desalination (AD) cycle with internal heat recovery between the condenser and the evaporator. A mathematical model of the AD cycle was developed and the performance data were compared with the experimental results. The advanced AD cycle is able to produce the specific daily water production (SDWP) of 9.24 m^3/tonne of silica gel per day at 70°C hot water inlet temperature while the corresponding performance ratio (PR) is comparatively high at 0.77. It is found that the cycle can be operational at 50°C hot water temperature with SDWP 4.3. The SDWP of the advanced cycle is almost twice that of the conventional AD cycle.

Keywords: Adsorption, desalination, waste heat, heat recovery

Nomenclature

A	total area (m^2)
c_p	specific heat capacity (J/kg·K)
D_{so}	kinetic constant for the silica gel water system (m^2/s)
E	characteristic energy (kJ/mole)
E_a	the activation energy (kJ/kg)
h_f	sensible heat (J/kg)
h_{fg}	latent heat of vaporization or condensation (J/kg)
M	mass (kg)
$\dot{m}$	mass flow rate (kg/s)
n	D-A constant (-)
P	pressure (Pa)
PR	performance ratio (-)
q	fraction of vapour adsorbed by the adsorbent (kg/kg of silica gel)
Q	power (W)
q_0	maximum adsorbed amount (kg/kg of silica gel)
$q*$	equilibrium uptake (kg/kg of silica gel)
Q_{st}	isosteric heat of adsorption (J/kg)
R	gas constant (J/kg mol)
R_p	particle radius (mm)
$SDWP$	specific daily water production (m^3 per tonne of silica gel per day)
t	time (s)
T	temperature (°C)
U	overall heat transfer coefficient ($W/m^2 \cdot K$)
v	specific volume (m^3/kg)
τ	number of cycles per day (-)

Subscripts

abe	adsorbate
ads	adsorber
chilled	chilled water
cond	condenser
cw	cooling water
cycle	one cycle with one bed undergoing either complete adsorption and desorption
d	distillate
des	desorber
evap	evaporator
hw	hot water

HX	heat exchanger
in	inlet
out	outlet
s	sea water
sg	silica gel
switching	switching period

1. Introduction

Potable water is a necessity for daily consumption and activities of human as well as the economic growth through the industrial processes. The accessible fresh water on Earth is less than 1% of the available water since 97% of the available water is either seawater or brackish water where the total dissolved solids (TDS) are more than 35 ppt. Within the fresh water inventory, as much as 65% is locked in the ice-caps or stored in deep aquifers under the ground surface. The water consumption by humans would double in every 20 years as the population growth rate increases. In the 2nd UN World Water Development Report, more than one billion people lack accessibility to safe drinking water, and 40 percent lack water for basic sanitation [1]. It is noted that over the past century, the global water consumption level has increased by tenfold, reaching or exceeding the limits of renewable water resources in some water stressed countries, such as in the Middle East, city states and North African countries. For instance, fresh water resources are almost completely exhausted in many middle-east region countries [2-5].

Desalination has become a practical solution for the global water shortage problem as its economic viability has improved drastically in recent decades. Worldwide, more than 15,000 industrial-scale desalination units have been installed or constructed. These plants account for a total capacity of 8.5 billion gallons of water/day [6]. The process of producing potable water by desalting of sea or brackish water can be classified into two main groups; namely (i) thermally-activated systems and (ii) pressure-driven systems. The International Desalination association (IDA) data shows that the reverse osmosis (RO) and multi-stage-flash (MSF) desalination processes account for 44% and 40% of the global installed desalting capacity, respectively [7]. However, these desalination processes have shortcomings such as high energy intensive, fouling in the separation units (membrane and evaporator) and high

operation cost. Being energy intensive, they contribute to environmental pollution such as global warming and green house gas emission through the burning of fossil fuels.

Over the last 200 years, a significant contribution by anthropogenic emission of greenhouse gases from the burning of fossil fuels has increased the atmospheric temperature by about 1.2 to 1.4ºF [8], contributing to the increasing melting rate of polar ice caps. Global warming has been increasing the melting rate of sea ice. Data from the National Ice and Snow Data Center (NISDC) showed that Arctic sea ice has declined dramatically over at least the past thirty years [9]. If the ocean surface receives a layer of fresh water, thermohaline circulation that contributes to a proper temperature balance across the earth can be disrupted [10]. Hence, the re-utilization or the conversion of waste heat to useful effects plays a crucial role in slowing down the global warming. Thus, the development of desalination technologies coupled with renewable energy sources or process waste heat has become indispensable [11].

Several studies have contributed to the desalination technologies that utilize renewable energy sources ranging from solar to geothermal energy [12-17]. The earliest development on adsorption-based desalination was reported by Broughton [18], using an ion-retarded resin for the vapor uptake, where a process with a thermally-driven two-bed configuration is simulated. Similar theoretical studies on the adsorption desalination plant were also proposed recently by Zejli et al. [19] and Al-kharabsheh and Goswami [20]. Solar heat source was studied as a heat source for the desalination plant, combined with an open-cycle adsorption heat pump using the zeolite as the adsorbent. Wang and Ng investigated the performance of the AD cycle using a four-bed regeneration scheme and reported the optimal specific daily water production (SDWP) of 4.7 kg/kg silica gel [21]. The operation strategy of the adsorption desalination plant has been reported highlighting the existence of the optimal cycle time depending on the regeneration temperatures [22]. The same authors have reported the performance of low temperature waste heat-driven adsorption desalination cum cooling cycles [23-25].

The motivation of the present study is to enhance the performance of the conventional multi-bed adsorption desalination cycle by incorporating internal heat recovery within part of the AD cycle, namely the evaporator-condenser units by having a coolant “run-around” circuit. The performance of the retrofitted AD desalination cycle is compared with the conventional AD cycle at similar ranges of the heat source, coolant and chilled water temperatures and flow rates as well as varying half-cycle time.

2. Description of the advanced AD cycle with the condenser/evaporator heat recovery circuit

The schematic diagram of the advanced AD cycle that employs the internal heat recovery between the condenser and the evaporator by a heat recovery circuit is shown in Figure 1. The AD cycle comprises an evaporator, a condenser, and four adsorber/desorber heat exchangers. The experimental AD plant was designed with the flexibility to operate either two-bed or four-bed operation mode. In the present study, the AD plant is investigated under two-bed operation mode where two physical adsorbers are under adsorption process while the other two beds perform as desorbers. The de-aerated sea water is evaporated in the evaporator where the water vapours are adsorbed on the surfaces of the adsorbent packed in the adsorber bed which is in communication with the evaporator through vapour pipe. The adsorption process is an exothermic process and thus, cooling is needed to maintain the temperature of the adsorbent so as to maximise the vapour uptake. For potable water conservation, cooling tower may use either the brackish or the seawater as the medium for heat rejection. The coolant used in the AD cycle during adsorption processes is isolated from the cooling tower water, namely the brackish or seawater, via an heat exchanger. The water vapours from the adsorber bed which is previously in adsorption mode are removed using low temperature hot water, typically below 85°C. The regenerated vapours from the desorber are condensed on the surfaces of the condenser tubes and condensate is collected as potable water. These evaporation-adsorption and desorption-condensation process are controlled by the cycle time.

In the advanced adsorption desalination (AD) cycle, the energy rejected at the condenser is recovered for the evaporation of the saline water in the evaporator. This internal heat recovery is achieved by the implementation of the heat transfer circuit that runs across the condenser and the evaporator of the AD cycle.

In the advanced AD cycles, the advantages over the conventional cycle are (i) the recovery of the condensation energy and its utilization for evaporation of the sea water, (ii) saving in the pumping power requirement for the condenser cooling water, and (iii) the increase in the pressure of adsorption process is a result of a higher evaporator temperature caused by the recovery of condenser heat.

3. Mathematical Modelling

Several mathematical models have been proposed for adsorption cooling cycles and can be found in open literatures [26-32]. The present mathematical modeling of a 2-bed advanced adsorption desalination cycle with the heat recovery between the condenser and the evaporator is developed based on adsorption isotherms, adsorption kinetics and energy balances between the sorption elements (adsorber/desorber heat exchangers), the evaporator and the condenser. Type-RD silica gel is employed as the adsorbent and the physical properties of type-RD silica gel are listed in Table 1. Dubinin–Astakhov (D-A) equation is used for the calculation of the water vapour uptake by the silica gel at specific temperature and pressure and is given by,

$$q^* = q_0 \exp\left[-\left(\frac{RT}{E}\ln\left(\frac{P}{P_0}\right)\right)^n\right] \tag{1}$$

where, q_0 is the maximum adsorbed amount, E is the characteristic energy and n is the surface heterogeneity parameter.

The transient uptake of by the silica gel can be obtained by linear driving force equation as,

$$\frac{dq}{dt} = \frac{15 D_{s0} \exp\left(\frac{-E_a}{RT}\right)}{R_p^{\,2}}\left(q^* - q\right) \tag{2}$$

where D_{so} is the kinetic constant for the silica gel water system, E_a is the activation energy, R_p is the particle radius and q denotes the instantaneous uptake.

It is assumed that the adsorbed and desorbed amounts of water vapour during the adsorption and desorption are the same and the overall mass balance of the cycle is given by,

$$\frac{dM_{s,evap}}{dt} = \dot{m}_{s,in} - \dot{m}_{d,cond} - \dot{m}_b \tag{3}$$

Here, $M_{s,evap}$ is the amount of sea water in the evaporator, $\dot{m}_{s,in}$ is the rate of feed sea water, $\dot{m}_{d,cond}$ is the mass of potable water extracted from the condenser and $\dot{m}_b$ is the mass of concentrated brine rejected from the evaporator. The energy balance of the evaporator in communication with the adsorbers is written as,

$$\begin{aligned}&\left[c_{p,s}\left(T_{evap}\right)M_{s,evap}+M_{HX,Evap}\ c_{pHX}\right]\frac{dT_{evap}}{dt}=h_f\left(T_{evap}\right)\dot{m}_{s,in}-\\&h_{fg}\left(T_{evap}\right)M_{sg}\left(\frac{dq_{ads}}{dt}\right)+\dot{m}_{evap}\ c_{p,evap}(T_{chilled,in}-T_{chilled,out})\end{aligned} \tag{4}$$

Similarly, the energy balance of the condenser is given by,

$$\begin{aligned}&\left[c_p\left(T_{cond}\right)M_{cond}+M_{HX,Cond}\ c_{pHX}\right]\frac{dT_{cond}}{dt}\\&=-h_f\left(T_{cond}\right)\frac{dM_d}{dt}+h_{fg}\left(T_{cond}\right)M_{sg}\left(\frac{dq_{des}}{dt}\right)\\&+\ \dot{m}_{cond}c_{p,cond}\left(T_{cond,in}-T_{cond,out}\right)\end{aligned} \tag{5}$$

In this cycle, $\dot{m}_{cond}=\dot{m}_{evap}$ since water re-circulating circuit is employed across the evaporator and the condenser for heat recovery.

The energy balance of the adsorber/desorber is given by,

$$\begin{aligned}&\left(M_{sg}c_{p,sg}+M_{HX,Ads}c_{p,HX}+M_{abe}c_{p,a}\right)\frac{dT_{ads/des}}{dt}=\pm Q_{st}\left(T_{ads/des},P_{evap/cond}\right)\\&n\times M_{sg}\frac{dq_{ads/des}}{dt}\pm\dot{m}_{cw/hw}\ c_{p,cw/hw}\left(T_{ads/des}\right)\left(T_{cw/hw,in}-T_{cw/hw,out}\right)\end{aligned} \tag{6}$$

where *n* is the number of adsorber or desorber bed in the cycle. In this analysis, the value of *n* is 2 since a pair of two reactors is under adsorption process whilst the other pair is under desorption mode. The specific heat capacity c_p is calculated as a function of adsorber temperature (T_{ads}) or desorber temperature (T_{des}) during adsorption or desorption process, respectively. Here Q_{st} stands for the isosteric heat of adsorption which is calculated [33-34] as follow,

$$Q_{st}=h_{fg}+E\left\{-\ln\left(\frac{q}{q_m}\right)\right\}^{1/n}+Tv_g\left(\frac{\partial P}{\partial T}\right)_g \tag{7}$$

where v_g is the specific volume of the gaseous phase, h_{fg} is the latent heat.

The outlet temperature of the water from each heat exchanger is estimated using log mean temperature difference method and it is given by,

$$T_{out} = T_0 + (T_{in} - T_0)\exp\left(\frac{-UA}{\dot{m}c_p(T_0)}\right) \tag{8}$$

Here T_0 is the temperature of the heat exchanger assuming uniform temperature across the reactor heat exchanger. In the advanced AD cycle where the heat recovery between the evaporator and the condenser is achieved by the heat recovery loop that circulates the water in between them. In this case, the outlet water from the evaporator is channelled to the inlet of the condenser whilst the outlet water from the condenser is sent to the evaporator.

The energy required to remove water vapors from the silica gels, (Q_{des}), can be calculated by using the inlet and outlet temperatures of the heat source supplied to the reactors, and this is given by,

$$Q_{des} = \dot{m}_{hw}c_{p,hw}(T_{hw})(T_{hw,in} - T_{hw,out}) \tag{9}$$

where $\dot{m}_{hw}$ indicates the mass flow rate and $c_{p,hw}$ defines the specific heat capacity of heating fluid. Concomitantly, the energy rejected to the cooling water during the adsorption process is estimated by the inlet and outlet temperatures of cooling fluid supplied to the other reactor and this is written as,

$$Q_{ads} = \dot{m}_{cw}c_{p,cw}(T_{cw})(T_{cw,out} - T_{cw,in}) \tag{10}$$

where $\dot{m}_{cw}$ and $c_{p,cw}$ indicate the mass flow rate and the specific heat capacity of cooling fluid. At the same time, the heat of evaporation (Q_{evap}), and the condensation energy (Q_{cond}) rejected at the condenser are given by,

$$Q_{evap} = \dot{m}_{evap}c_{p,evap}(T_{evap})(T_{chilled,in} - T_{chilled,out}) \tag{11}$$

$$Q_{cond} = \dot{m}_{cond}c_{p,cw}(T_{cond})(T_{cond,out} - T_{cond,in}) \tag{12}$$

It is noted that the roles of the reactors for adsorption or desorption are switched in a half-cycle time.

Finally, the performance of the advanced adsorption desalination cycle is assessed in terms of specific daily water production (SDWP) and the performance ratio (PR) as follows,

$$SDWP = \int_0^{t_{cycle}} \frac{Q_{cond}\,\tau}{h_{fg}(T_{cond})M_{sg}}\,dt \tag{13}$$

$$PR = \int_0^{t_{cycle}} \frac{\dot{m}_{water} h_{fg}(T_{cond})\tau}{Q_{des}}\,dt \tag{14}$$

In this cycle, t_{cycle} is the duration of the adsorption and desorption processes whilst $t_{switching}$ is the time for which the adsorber and desorber beds change their roles. The mathematical modeling equations of the advanced adsorption desalination are solved using the Gear's BDF method from the IMSL library linked by the simulation code written in FORTRAN Power Station, and the solver employs a double precision with tolerance value of $1x10^{-6}$. Table 2 furnishes the parameters used in the simulation program.

4. Results and discussions

The performance of the advanced adsorption cycle with the internal heat recovery between the evaporator and the condenser is experimentally investigated. The pilot AD plant has been constructed and the heat recovery circuit is implemented between the condenser and the evaporator. Figure 2 depicts the pictorial view of the advanced AD plant showing the condenser-evaporator heat recovery circuit.

The transient temperature profiles of the major components of the advanced AD cycle that incorporates the heat recovery scheme between the condenser and the evaporator are shown in Figure 3. In this analysis, the hot water inlet temperature was maintained at 70°C while the cycle time (t_{cycle}) and the switching time ($t_{switching}$) are kept 600s with 40s, respectively. It is noted that the experimental temperature measurements are subjects to the time constant of the sensors. As can be observed from Fig. 3, the simulated results of transient temperature agree

well with those of the experimental data thus the simulation is being validated by the experiment.

The hysteretic found in the condenser temperature is resulted from the location of the sensor which is placed near the desorber vapour pipe. Thus, it fails to capture the temperature drop by the cold front from the evaporator at the beginning of the cycle operation.

The temperature profiles of the inlet and outlet water of the heating and cooling fluids for 55°C hot water inlet temperature are shown in the Fig. 4. It is found that there is a large fluctuation in the hot and cooling water outlet temperatures during the switching period where the pre-heating of the adsorber and the pre-cooling of the desorber reactors are taking place.

It can also be observed from Fig. 4 that the temperature differences between the evaporator outlet and the condenser inlet, and that between the condenser outlet and the evaporator inlet are negligibly small resulted from the good thermal insulation of the pipes involved in the heat recovery circuit between the condenser and the evaporator.

The parametric study of the advanced AD cycle has been conducted to investigate the performance of the cycle under various operating conditions. The cycle is studied under different hot water inlet temperatures, selectively between 50°C and 70°C, which is the practical available temperature range that can be recovered from the low temperature waste heat or solar energy. Figure 5 gives the specific daily water production (SDWP) and the performance ratio (PR) of the advanced AD cycle while operating at different hot water inlet temperatures. The experimental results show that the SDWP linearly increases with the hot water inlet temperature and is about 9.24 m^3 per tonne of silica gel per day at 70°C hot water inlet temperature, whilst the SDWP reaches 14.2 m^3 per tonne of silica gel per day at 85°C hot water inlet temperature.

The increase in the SDWP with the increase in the hot water temperature is attributed to the better desorption-condensation process at higher regeneration temperatures resulting in the increase in SDWP. It should be noted that the advanced AD cycle is capable to operate at substantially low hot water inlet temperature i.e., 50°C at which conventional AD cycle fails to operate and the produced SDWP is 5.2 m^3 of potable water per tonne of silica gel per day.

It can be seen from Fig. 5, the performance ratio (PR) of the plant remains relatively constant with the regeneration temperature due mainly to the resilience of silica gel with water vapor. At 85°C hot water inlet temperature, the SDWP of the advanced AD cycle is found to be 13.5 which is twice that achieved by the conventional AD cycle [24].

The effect of the cooling water inlet temperature on the performance of the advanced AD cycle is shown in Figure 6. The SDWP of the cycle for two sets of hot water inlet temperatures i.e., 70°C and 50°C is presented while varying the temperature of the coolant from 26°C to 32°C. Higher water production rate is achieved at lower coolant temperatures while the production rate decreases as increased in the coolant temperature.

The performance of the advanced AD cycle under different flow rates of the heating and cooling fluids is presented in Figures 7 to 9. It is found that the SDWP of the cycle increases with the increase in the flow rate while the temperature of heat source and cooling temperatures are held at 70°C and 30°C, respectively. The performance improvement is attributed to the better heat transfer coefficient at higher flow rates.

The effect of hot water flow rates on SDWP for four different flow rates of cooling water is depicted in Figure 7. SDWP increases only moderately with the increase in hot water flow rates.

Figure 8 gives the SDWP of the advanced AD cycle for assorted cooling water flow rates at specific hot water flow rate and constant hot water inlet temperature at 70°C. The results showed that the water production rate increased at higher cooling flow rates. This is due to the improvement in the heat transfer coefficient at higher flow rates. It is also noted that the increase in the SDWP becomes less significant at flow rates higher than 1.67 kg/s due to finite amount of adsorption and desorption capacities of the adsorbent.

The performance of the advanced AD cycle under different flow rates of the heating and cooling fluids is presented in Figure 9. The liner increment in the SDWP is observed while the temperature of heat source and cooling temperatures are held at 70°C and 29°C, respectively.

It has been reported that the cycle time at which the AD cycle provides the optimal potable water production varies with the available hot water inlet temperatures [23]. The optimal cycle times for the advanced AD cycle have been experimentally evaluated for two different temperature levels of hot water and are shown in Figure 10. The results showed that the

optimal cycle times exist at the half-cycle time 570s and 600s for 70°C and 65°C, respectively whilst the corresponding SDWPs are 9.39 and 8.3. The optimal cycle time for the advanced AD cycle is shorter than that of the conventional AD cycle [23].

This is because the evaporation-adsorption and desorption-condensation processes in the advanced AD cycle become much faster due to the pressurization of the adsorption and the lower in the condensation temperature resulted from the heat recovery process between the condenser and the evaporator. The pressurization of the adsorption process is achieved since the relatively higher temperature water from the condenser is utilized for the evaporation. On the other hand, the temperature of the outlet water from the evaporator that is channelled to the condenser is around 25°C to 27°C and this cold front lower condensing temperature imparts the better desorption process. These effects are more significant at the beginning of the operation mode after switching process since the adsorption and desorption rates at maximum at that period.

5. Conclusions

A significant improvement in the performance of the advanced AD cycle is recorded with internal heat recovery between the condenser and the evaporator. These findings are also predicted to agree well with the experiments. For this configuration, the maximum specific daily water production (SDWP) of the AD cycle is about 9.34 m^3 of potable water per tonne of silica gel per day at a regeneration temperature of 70°C and the corresponding performance ratio is 0.77 which implies that the AD cycle is an efficient cycle. The experimental results showed that it can operate even at a low hot water inlet temperature as low as 50°C and yet is delivering a respectable SDWP of 5.5. The optimal cycle time of the advanced cycle has been evaluated to be shorter than that of a conventional AD cycle.

Acknowledgements

The authors' gratefully acknowledge the financial support given by grants (No. R33-2009-000-101660) from the World Class University (WCU) Project of the National Research Foundation, (R265-000-286-597) from King Abdullah University of Science and Technology (KAUST) and (R265-000-287-305) from ASTAR.

REFERENCES:

[1]. The 2nd United Nations World Water Development Report, 2006, 'Water, a shared responsibility'.

[2]. M. Schiffler, Perspectives and challenges for desalination in the 21st century, Desalination, 165 (2004) 1-9.

[3]. Seminth Otles and Serkan Otles, Desalination techniques, EJEAFChe, 4(4), 963-969, 2004.

[4]. Durham Sustain Availability, Environmental Sustainability Program Ontario, at http://www.sustainability.ca/index.cfm?body=chunkout.cfm&k1=403

[5]. Mohamed A. Eltawil, Zhao Zhengming, Liqiang Yuan, A review of renewable energy technologies integrated with desalination systems, Renewable and Sustainable Energy Reviews 13 (2009) 2245–2262.

[6]. Ebensperger U, Isley P. Review of the current state of desalination: water policy working paper 2005-008.

[7]. IDA. IDA worldwide desalting inventory 2002. International Desalination Association; 2002.

[8]. http://www.epa.gov/climatechange/basicinfo.html

[9]. http://nsidc.org/arcticseaicenews/index.html

[10]. http://nsidc.org/seaice/environment/global_climate.html

[11]. S. A. Kalogirou, Seawater desalination using renewable energy sources, Progress in Energy and Combustion Science, 31 (2005) 242–281.

[12]. Delyannis EE, Status of solar assisted desalination: a review, Desalination 1987; 67:3–19.

[13]. Garcia-Rodriguez L, Gomez-Camacho C, Perspectives of solar desalination, Desalination 2001; 136:213–8.

[14]. Belessiotis V, Delyannis EE, The story of renewable energies for water desalination, Desalination 2000; 128:147–59.

[15]. Delyannis EE, Belessiotis V, A historical overview of renewable energies, In: Mediterranean conference on renewable energy sources for water production. European Commission, EURORED Network, CRES, EDS; 1996. p. 13–7.

[16]. Mathioulakis E, Belessiotis V, Delyannis E, Desalination by using alternative energy: review and state-of-the-art, Desalination 2007; 203:346–65.

[17]. G. Fiorenza, V.K. Sharma, G. Braccio, Techno-economic evaluation of a solar powered water desalination plant, Energy conversion and Management 44 (2003) 2217-2240.

[18]. D.B. Broughton, Continuous desalination process, USPO 4,447,329, May 8, 1984

[19]. D. Zejli, R. Benchrifa, A. Bennouna, O.K. Bouhelal, A solar adsorption desalination device: first simulation results, Desalination 168 (2004) 127–135.

[20]. S. Al-kharabsheh, D.Y. Goswami, Theoretical analysis of a water desalination system using low grade solar heat, Journal of solar energy engineering transactions of the ASME 126 (2) (2004) 774–780.

[21]. X. Wang, K.C. Ng, Experimental investigation of an adsorption desalination plant using low-temperature waste heat, Applied Thermal Engineering, 25 (2005) 2780–2789.

[22]. I. I. EI-Sharkawy, K. Thu, K. C. Ng, B.B. Saha, A. Chakraborty, S. Koyama, 2007, Performance Improvement of Adsorption Desalination Plant: Experimental Investigation, Int. Review of Mech. Engrg.1.

[23]. K. Thu, K.C. Ng, B.B. Saha, A. Chakraborty and S. Koyama, "Operational strategy of adsorption desalination system", International Journal of Heat and Mass Transfer, Vol. 52, Nos. 7-8, pp. 1811-1816, 2009.

[24]. K.C. Ng, K. Thu, A. Chakraborty, B.B. Saha and W.G. Chun, "Solar-assisted dual-effect adsorption cycle for the production of cooling effect and potable water", International Journal of Low-Carbon Technologies, Vol. 4, 2009.

[25]. B.B. Saha, K.C. Ng, A. Chakraborty and K. Thu, Most Energy Efficient Approach of Desalination and Cooling, Cooling India, May-June, 2009, pp (72-78).

[26]. K. C. Ng, M. A. Sai, A. Chakraborty, B. B. Saha, S. Koyama, 2006, The electro-adsorption chiller: Performance rating of a novel miniaturized cooling cycle for electronics cooling, ASME Trans. J. Heat Trans., 128, 889.

[27]. B. B. Saha, A. Chakraborty, S. Koyama, K. C. Ng, M. A. Sai, 2006, Performance modeling of an electro-adsorption chiller, Philos. Magazine, 86, 3613.

[28]. A. Chakraborty, B. B. Saha, S. Koyama, K. C. Ng, K. Srinivasan, Adsorption Thermodynamics of silica gel – water system, J. Chem. Eng. Data, Article in press, 2008.

[29]. H. T. Chua, K. C. Ng, A. Malek, T. Kashiwagi, A. Akisawa, B. B. Saha, Multi-bed regenerative adsorption chiller-improving the utilization of waste heat and reducing the chilled water outlet temperature fluctuation, Int. J. Ref. 24 (2001) 124-136.

[30]. K.C. Ng, X. Wang, Y.S. Lim, B.B. Saha, A. Chakraborty, S. Koyama, A. Akisawa and T. Kashiwagi, Experimental study on performance improvement of a four-bed adsorption chiller by using heat and mass recovery, International Journal of Heat and Mass Transfer 49(19-20) (2006) 3343-3348.

[31]. B.B. Saha, K.C.A. Alam, A. Akisawa, T. Kashiwagi, K.C. Ng and H.T. Chua, Two-stage non-regenerative silica gel-water adsorption refrigeration cycle, ASME Advanced Energy Systems Division, Orlando 40 (2000) 65-69.

[32]. B.B. Saha, I.I. El-Sharkawy, A. Chakraborty and S. Koyama, Study on an activated carbon fiber-ethanol adsorption chiller: Part I — system description and modelling, International Journal of Refrigeration 30(1) (2007) 86-95.

[33]. Theory and experimental validation on isosteric heat of adsorption for an adsorbent + adsorbate system, Anutosh Chakraborty, Bidyut Baran Saha, Ibrahim I. El-Sharkawy, Shigeu Koyoma, Kandadai Srinivasan and Kim Choon Ng, High Temperatures-High Pressures, Vol. 37, pp. 109-117.

[34]. Theoretical Insight of Physical Adsorption for a Single-Component Adsorbent + Adsorbate System: I. Thermodynamic Property Surfaces, Anutosh Chakraborty, Bidyut Baran Saha, Kim Choon Ng, Shigeu Koyoma and Kandadai Srinivasan, Langmuir, 2009, 25 (4), 2204-2211.

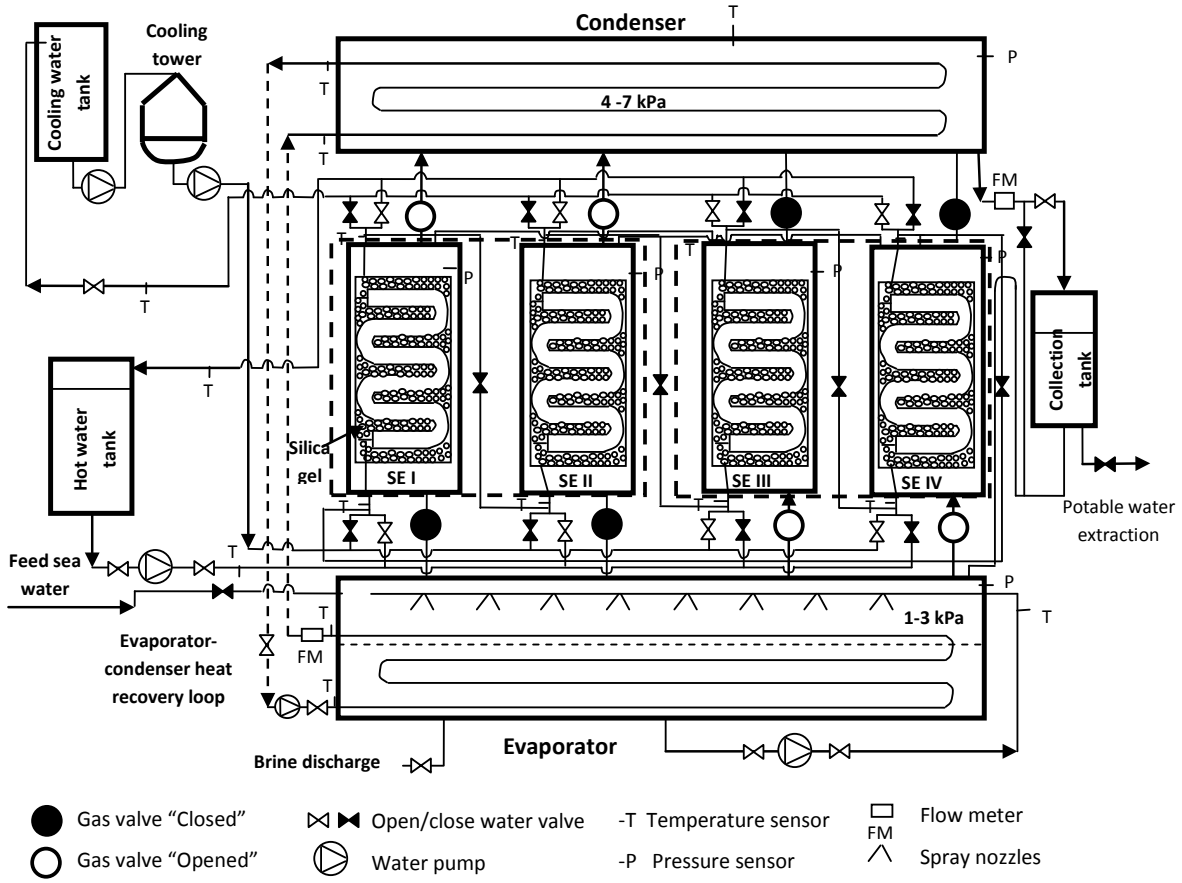

Figure 1. Schematic diagram of the advanced AD cycle with the evaporator-condenser heat recovery circuit.

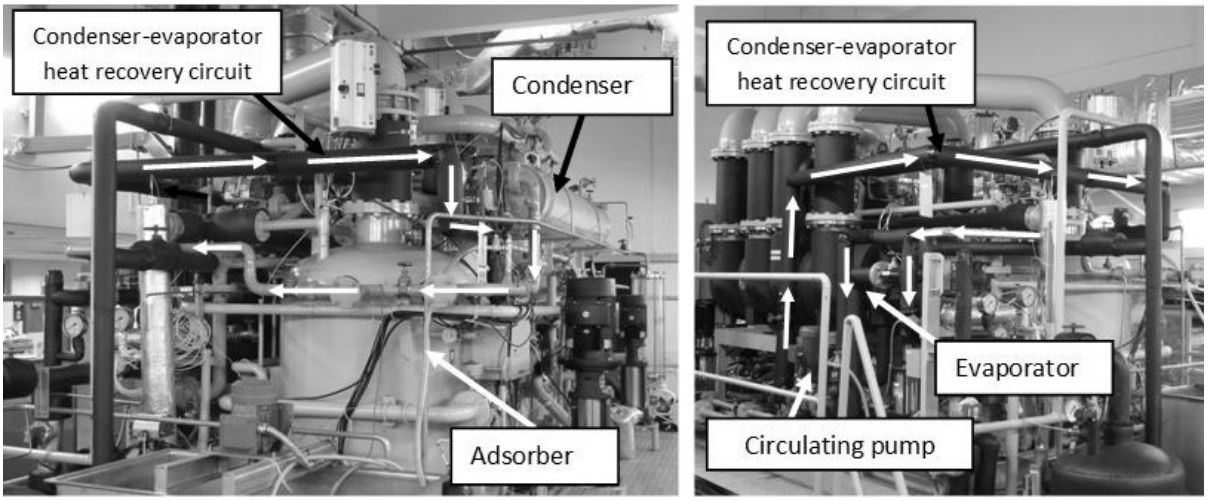

Figure 2. Pictorial view of the AD cycle with the condenser-evaporator heat recovery circuit.

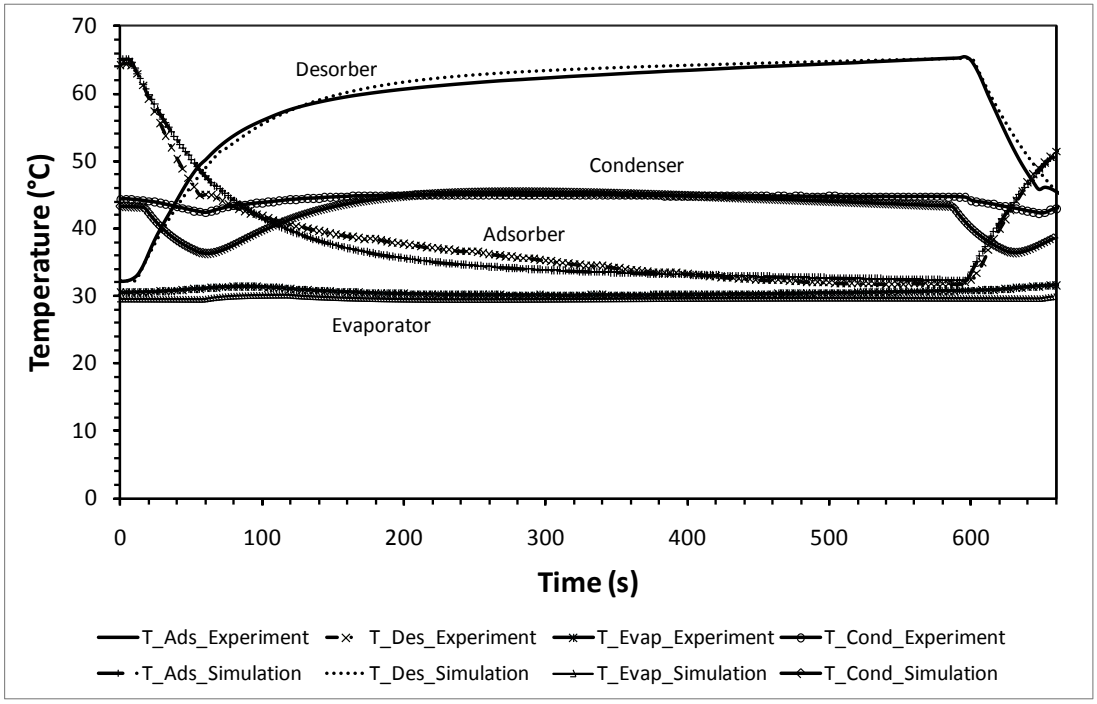

Figure 3. The temperature profiles of the major components of the advanced AD cycle.

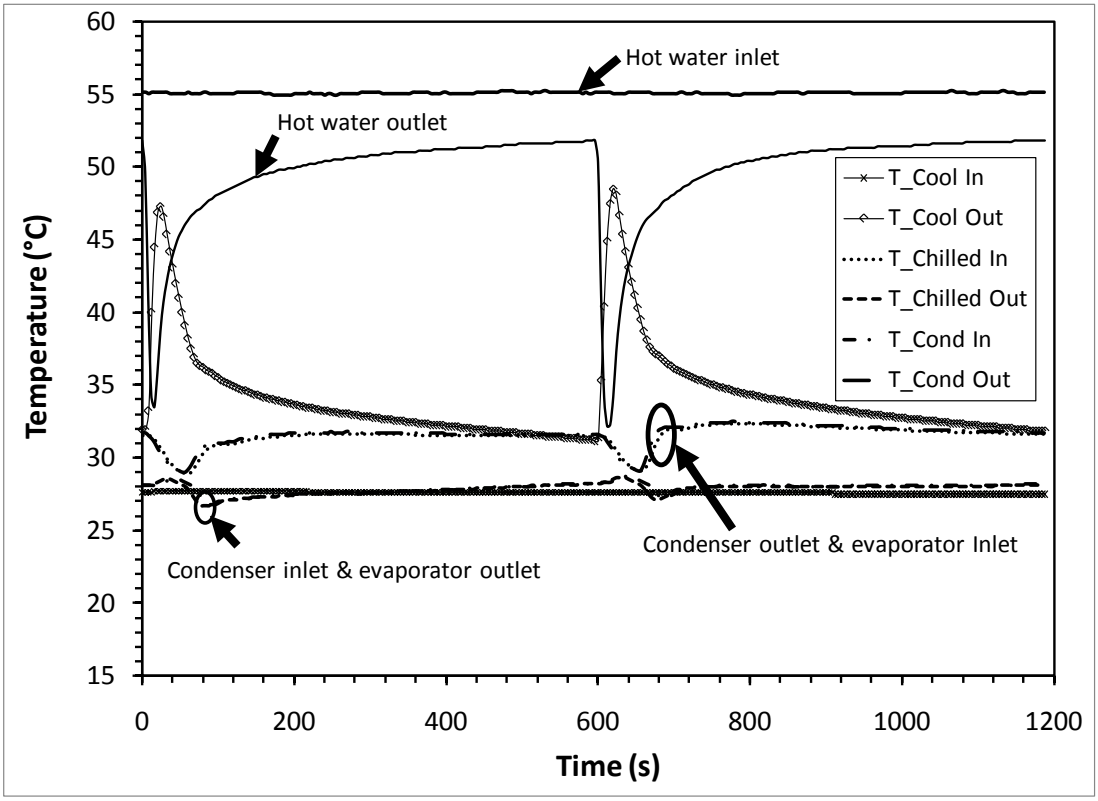

Figure 4. The temperature profiles of the inlet and outlet of the heat transfer fluids measured experimentally.

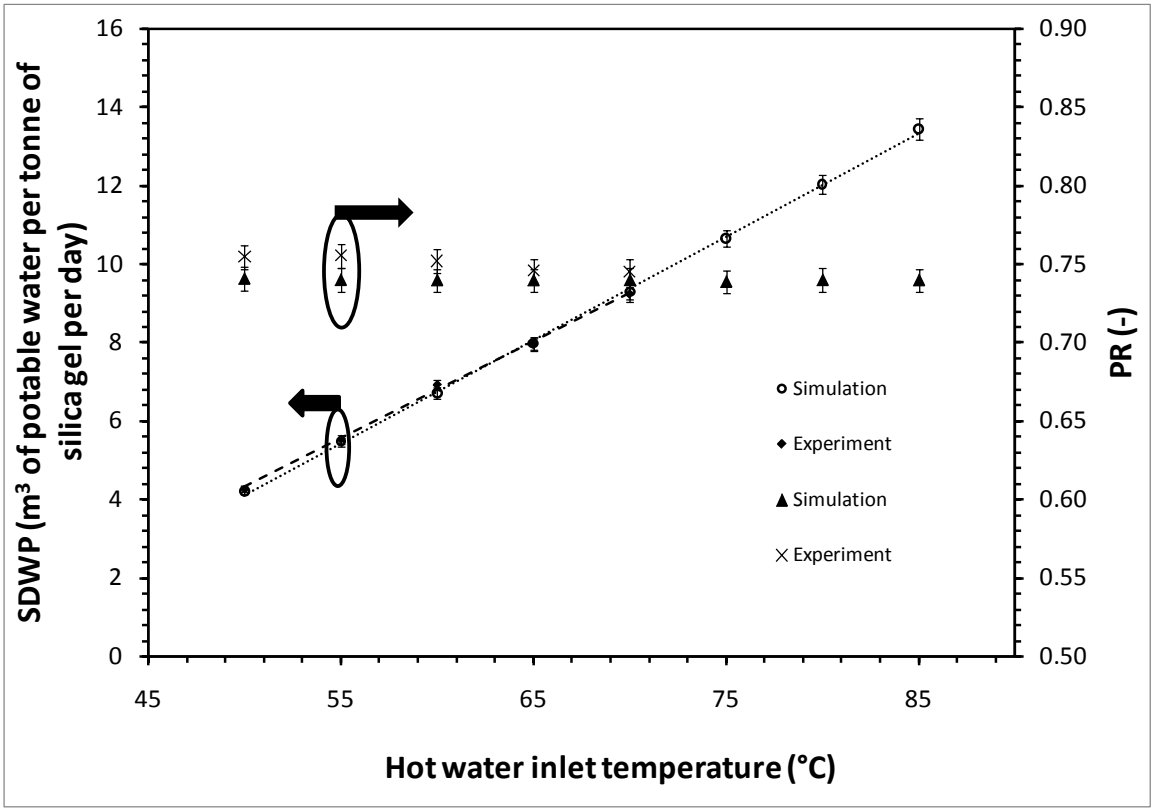

Figure 5. The SDWP and PR of the advanced AD cycle with assorted hot water inlet temperatures ranging from 50°C to 70°C.

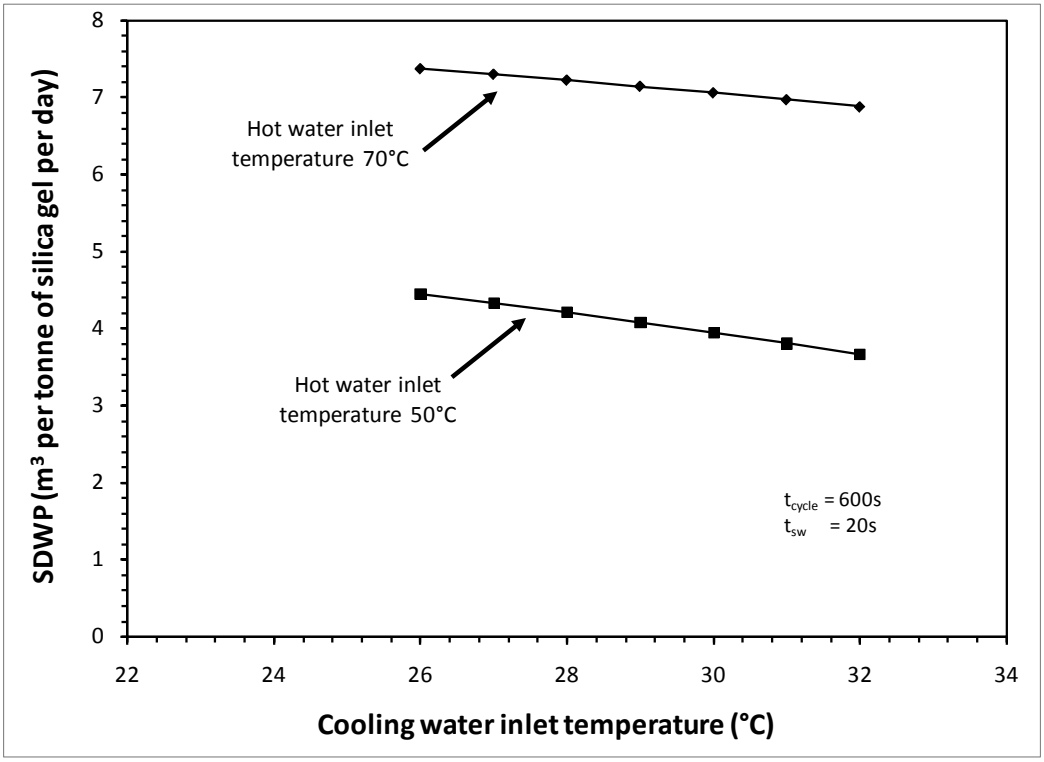

Figure 6. The performance of the advanced AD cycle at different cooling water inlet temperatures.

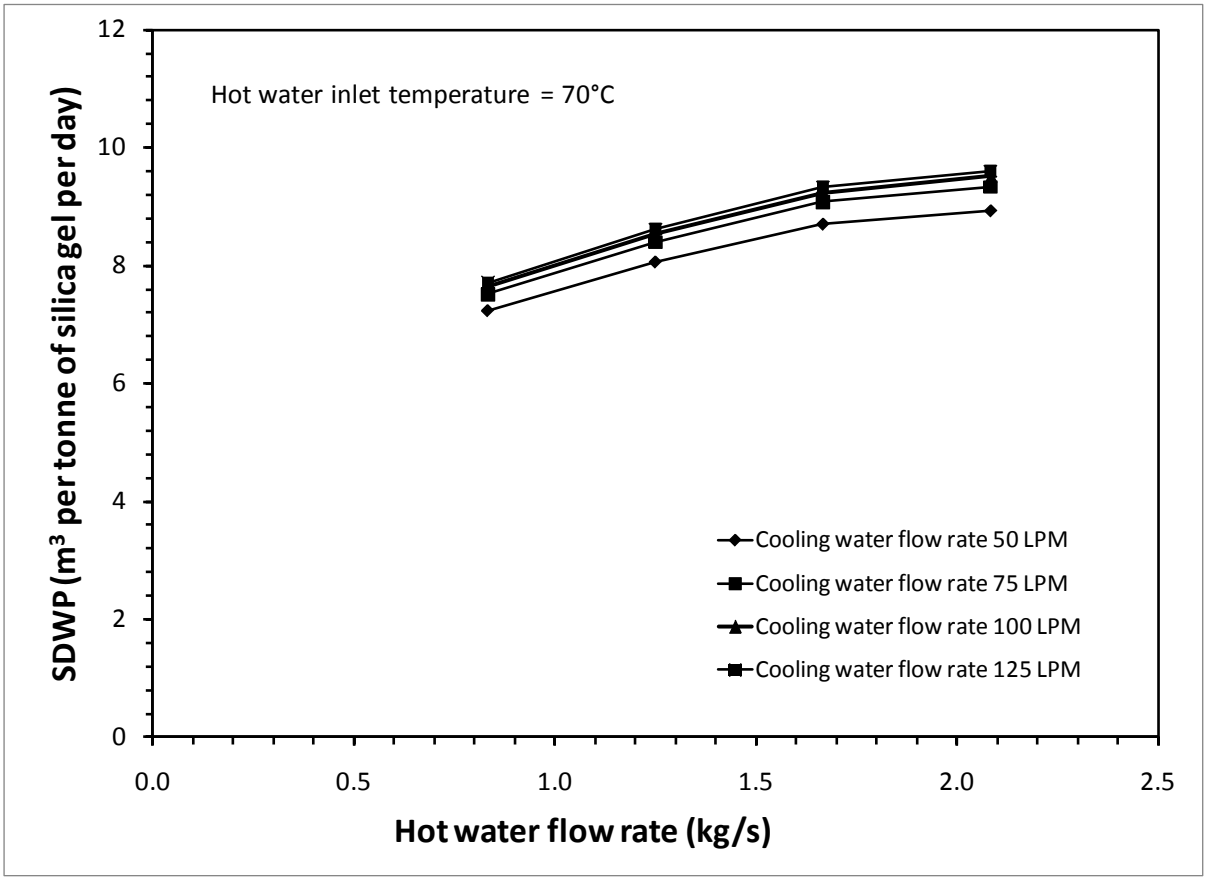

Figure 7. Specific daily water production of the advanced AD cycle for assorted hot water flow rates.

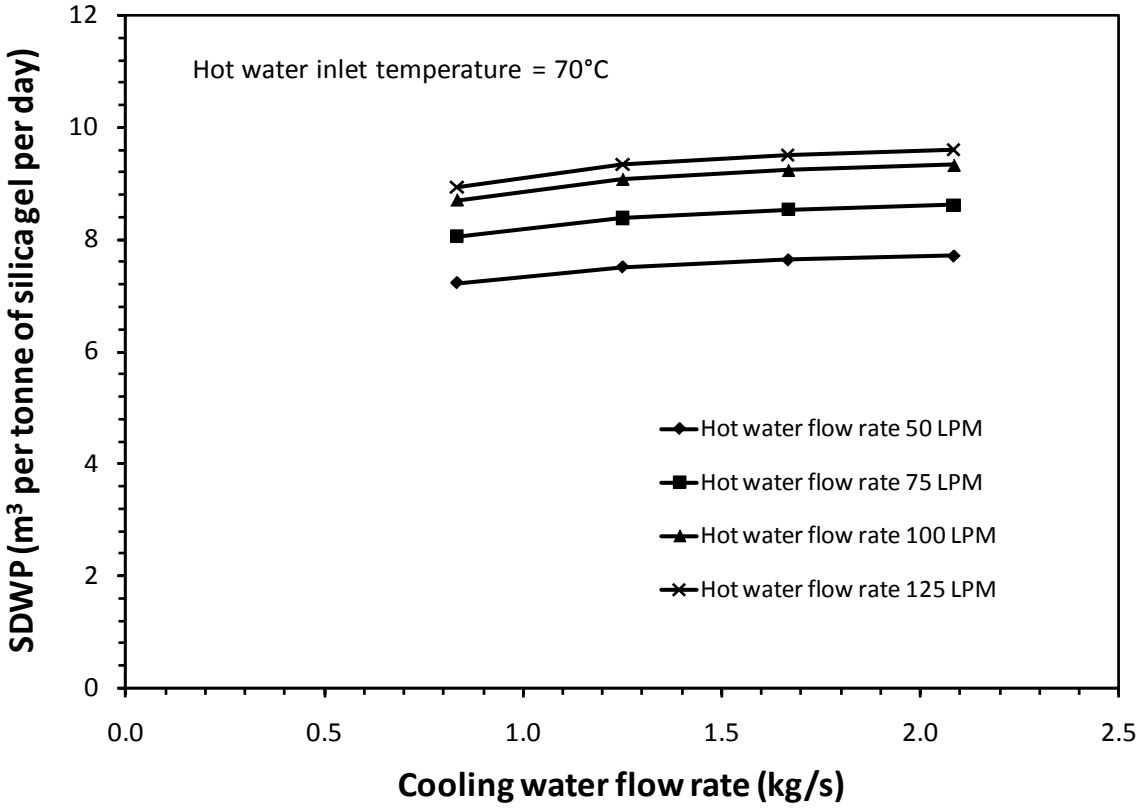

Figure 8. Specific daily water production of the advanced AD cycle for assorted cooling water flow rates.

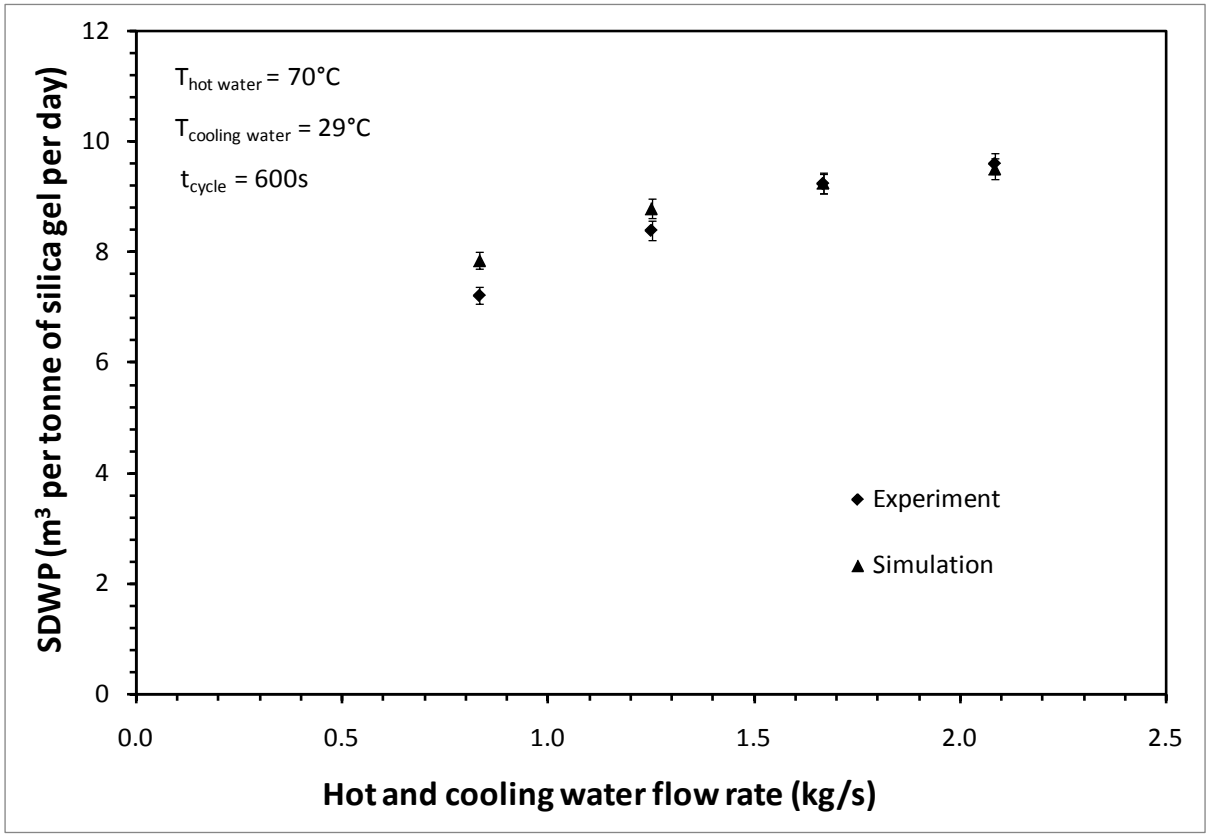

Figure 9. Performance of the advanced AD cycle using different flow rates of heating and cooling fluids at constant source temperatures.

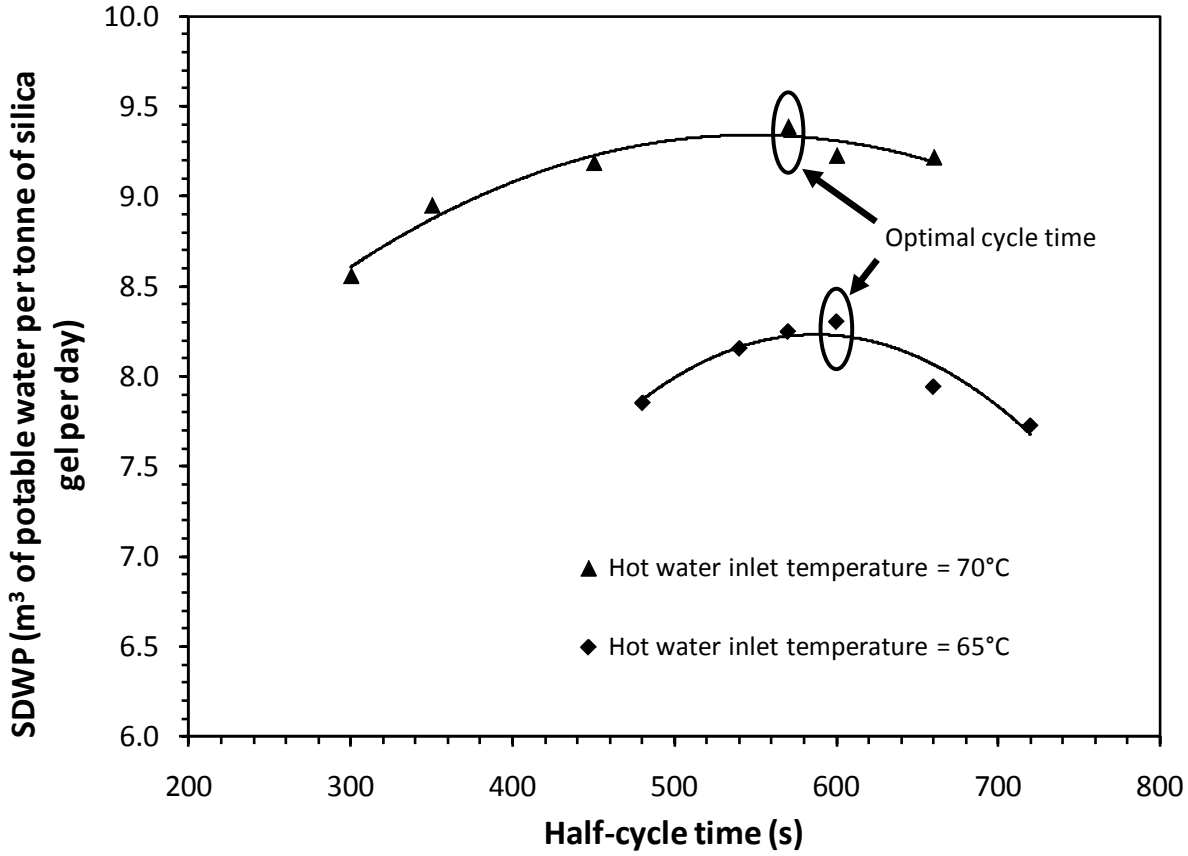

Figure 10. The performance of the advanced AD cycle showing the optimal cycle times at hot water inlet temperatures 70°C and 65°C.

Table 1. Physical properties of Type-RD silica gel.

Property	**Value**
Pore size (nm)	0.8-7.5
Porous volume (cm^3/g)	0.37
Surface area (m^2/g)	720
Average pore diameter (nm)	2.2
Apparent density (kg/m^{-3})	700
pH (-)	4.0
Specific heat capacity (kJ/kg·K)	0.924
Thermal conductivity (W/m·K)	0.198

Table 2. Values of the parameters used in the simulation program.

Parameter	**Value**
q_0	0.592 (kg/kg of silica gel)
E	3.105 (kJ/mole)
n	1.1 (-)
D_{so}	2.54×10^{-4} (m^2/s)
E_a	4.2×10^{-4} (kJ/kg)
R_p	0.4 (mm)
$T_{hw,in}$	50-85 (°C)
$T_{cw,in}$	30 (°C)
M_{sg}	36 (kg)
A_{bed}	41.7 (m^2)
$M_{HX,Ads}\ c_{p,HX}$	184.1(kJ/K)
$M_{HX,Evap}\ c_{p,HX}$	25.44 (kJ/K)
$M_{HX,Cond}\ c_{p,HX}$	12.62 (kJ/K)
U_{ads}	250 ($W/m^2 \cdot K$)
U_{des}	240 ($W/m^2 \cdot K$)
A_{evap}	3.5 (m^2)
A_{cond}	5.08 (m^2)
$c_{p,sg}$	924 (J/kg·K)
t_{cycle}	600 (s)
$t_{switching}$	40 (s)
$\dot{m}_{cw}, \dot{m}_{hw}$	0.83-2.08 (kg/s)
$\dot{m}_{chilled} = \dot{m}_{cond}$	1.42 (kg/s)